

Bottlebrush Polymers

How to cite:

International Edition: doi.org/10.1002/anie.202217941

German Edition: doi.org/10.1002/ange.202217941

Circular Upcycling of Bottlebrush Thermosets

Daixuan Zhang⁺, Foad Vashahi⁺, Erfan Dashtimoghadam, Xiaobo Hu, Claire J. Wang, Jessica Garcia, Aleksandra V. Bystrova, Mohammad Vatankhah-Varnoosfaderani, Frank A. Leibfarth, and Sergei S. Sheiko*

Abstract: The inability to re-process thermosets hinders their utility and sustainability. An ideal material should combine closed-loop recycling and upcycling capabilities. This trait is realized in polydimethylsiloxane bottlebrush networks using thermoreversible Diels–Alder cycloadditions to enable both reversible disassembly into a polymer melt and on-demand reconfiguration to an elastomer of either lower or higher stiffness. The crosslink density was tuned by loading the functionalized networks with a controlled fraction of dormant crosslinkers and crosslinker scavengers, such as furan-capped bis-maleimide and anthracene, respectively. The resulting modulus variations precisely followed the stoichiometry of activated furan and maleimide moieties, demonstrating the lack of side reactions during reprocessing. The presented circularity concept is independent from the backbone or side chain chemistry, making it potentially applicable to a wide range of brush-like polymers.

Introduction

Crosslinking of polymers into networks provides them with mechanical stability and dimensional integrity. These same covalent crosslinks that enhance material properties concurrently hinder the re-processing of products at their end-of-life.^[1–5] There are two general approaches to re-processing of polymers: recycling and upcycling, and both are intended to enhance sustainability while pursuing distinct conversion pathways and valorization targets. Closed-loop recycling technologies enable recreating the original material through a circular deconstruction-reconstruction, e.g., depolymerization-repolymerization process, thus creating a sustainable

substitute with a similar value.^[6–9] However, closed-loop recycling of crosslinked thermosets is not possible due to irreversible, covalent crosslinks.^[10–12] To provide end-of-life solutions for these recalcitrant materials, upcycling approaches have been developed involving polymer functionalization and/or depolymerization^[13–16] to convert a post-consumer product into a new material of higher value.^[16–23]

An ideal thermoset material would provide pathways for both upcycling and circularity, whereby a polymer network can be both reconfigured into a new product and/or reversibly disassembled to its constituent building blocks.^[24,25] The built-in circularity (by integrating closed-loop recycling and upcycling in one material) is difficult to realize in conventional thermosets given the irreversible crosslinks,^[12,26,27] but has been successfully implemented in dynamic networks such as vitrimers, allowing full recovery of monomer feedstocks for reprocessing.^[1,17,28–34] This approach can be further advanced by taking advantage of brush-like polymer architectures that constitute a distinct subset of polymer networks with unique properties, such as tissue-mimetic mechanics,^[35,36] enhanced swelling,^[37,38] and structural coloration.^[35,39] Brush-like polymers are already widely used in industrial products such as coatings and adhesives, while tissue-mimetic elastomers and gels with architecturally tunable mechanics open opportunities for the design of personalized biomedical devices. Unlike their linear counterparts, brush networks combine several advantageous characteristics: (i) the myriad of chain-end functionalities provide synthetic flexibility for both permanent and reversible crosslinking,^[40–42] (ii) the large size of bottlebrush strands allows for scaffold percolation with much fewer number of nodes, (iii) the lack of chain entanglements lowers melt viscosity and facilitates molding, and (iv) the extra free volume of chain ends enhances mobility of reagents during post-crosslinking chemical modification. The outlined capabilities allow constructing a re-processing triangle that incorporates both *reconfiguration* on demand and *recycling* to a reusable melt of functional bottlebrush mesoblocks (Figure 1). For example, one may start with constructing *Network 1* (high crosslink density) from *melt*, followed by its reconfiguration to *Network 2* (low crosslink density). Switching from stiff rubber to a tissue-mimetic material leads to value-added applications in biomedical devices and soft robotics. Alternatively, *N1* can be completely disassembled into bottlebrush *melt* to be re-crosslinked to *N2*. It is important to note that within this triangle, each product is stable for a long time and every transformation is reversible.^[41,43]

[*] Dr. D. Zhang,⁺ Dr. F. Vashahi,⁺ Dr. E. Dashtimoghadam, Dr. X. Hu, C. J. Wang, J. Garcia, Dr. M. Vatankhah-Varnoosfaderani, Prof. F. A. Leibfarth, Prof. S. S. Sheiko
 Department of Chemistry
 University of North Carolina at Chapel Hill
 Chapel Hill, NC 27599 (USA)
 E-mail: sergei@email.unc.edu

A. V. Bystrova

A.N.Nesmeyanov Institute of Organoelement Compounds of Russian Academy of Sciences, Vavilova St. 28, Moscow, 119334 (Russian Federation)

[†] These authors contributed equally to this work.

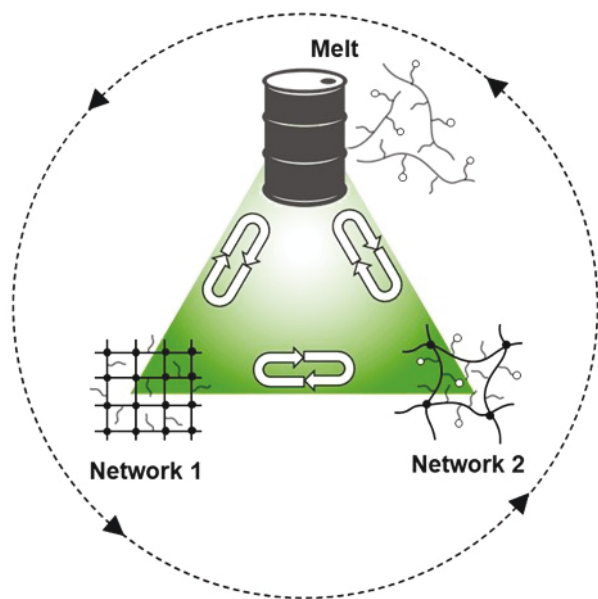


Figure 1. Upcycling of bottlebrush thermosets into circular materials. Bottlebrushes with a controlled fraction of reactive side-chain ends allow one-way yet reversible crosslinking, whereby materials at every state (melt or elastomer) remain infinitely stable until re-activation. The circularity is achieved by pre-loading elastomers with dormant crosslinkers or crosslinker scavengers that respectively increase (Network 2 to Network 1) or decrease the crosslink density (N1 to N2), including full network disassembly (N1 or N2 to Melt).

Results and Discussion

To demonstrate the feasibility of circular upcycling of bottlebrush networks, we use the thermoreversible Diels–Alder reactions (DA and retro-DA) through incorporation of furan (F) moieties at side chain ends and addition of bis-maleimide (bis-M) crosslinkers.^[13,33,44–46] DA chemistry has been successfully used for recycling of linear thermosets by providing stable covalent crosslinking at room temperature and controlled dissociation at higher temperatures.^[47–51] This reversible chemistry in conjunction with the aforementioned traits of brush architecture creates an intrinsic fluid-like environment to enable molecular mobility for reactions in a solvent-free state. Brush strands are synthesized through copolymerization of monomethacryloxypropyl terminated polydimethylsiloxane (PDMSMA, 1000 g mol⁻¹) and hydroxyl-terminated polyethylene glycol methacrylate (PEGMA, 500 g mol⁻¹) macromonomers via atom transfer radical polymerization (ATRP) (Figure 2A, see Supporting Information for synthetic details). The PEGMA fraction was kept under 10 wt.% to ensure miscibility with PDMSMA macromonomers. For a 600:1 monomer/initiator ratio, the degree of polymerization at 66.6% conversion is determined by ¹H NMR as $n_{bb} \cong 417$, which is consistent with $0.67 \times 600 = 402$ and number average $n_{bb} \cong 256$, $\bar{D} = 1.1$ and $n_{bb} \cong 303$, $\bar{D} = 1.12$ from multi-angle light-scattering gel-permeation chromatography (MALS-GPC) and molecular imaging with atomic force microscopy (AFM), respectively

(Supporting Information, Figures S1 and S14). Monitoring conversion of the two macromonomers over time confirmed random copolymerization (Supporting Information, Figure S2–3). Prior to functionalization, bottlebrush macromolecules were purified to remove residual monomers (Figure S1). The hydroxyl-terminated PEGMA ends are reacted with furfuryl isocyanate (FNCO) to produce bottlebrushes with a controlled fraction of F-functionalized side chains (2.65 mol% functionalization verified by ¹H NMR spectroscopy, Supporting Information, Figure S4). In parallel, a bis-maleimide PDMS crosslinker was synthesized to ensure miscibility with the PDMS side chains (Supporting Information, Figure S5).

Reversible assembly-disassembly of DA-crosslinked networks was monitored by measuring the storage and loss moduli as a function of temperature (T) and time (Figure 2B). At lower T , the M and F moieties react to produce a covalent bottlebrush network. The crosslinking demonstrates typical Arrhenius behavior, where the rate of the crosslinking reaction is lower at lower temperatures (Figure 2B inset). Upon heating, the network dissociates into a melt of PDMS bottlebrushes (Supplementary Videos 1 and 2). In the corresponding T sweeps, three distinct regions are identified: (i) at $T < 60^\circ\text{C}$, DA coupling reactions dominate over retro-DA, indicative of stable network where the crosslink density remains invariable, (ii) at $70 < T < 130^\circ\text{C}$, the DA and retro-DA reactions are in equilibrium, resulting in softening at $G' > G''$, which enables network upcycling while preserving its structural integrity, and (iii) at $T > 130^\circ\text{C}$, the retro-DA reaction is much faster than DA cycloaddition, which permits chemical recycling back to the bottlebrush precursor. Once the heat is removed, the DA cycloaddition converts the network to its original state (Supporting Information, Figure S6).^[46,52]

By varying the M/F feeding ratio, elastomers are obtained with different crosslink densities ($\approx n_x^{-1}$), where n_x is a backbone DP between DA crosslinks. These individual materials demonstrate the Young's modulus, E_0 , ranging from 2 to 20 kPa in tensile tests (Figure 2C and Figure S6). Elastomers made that contain a higher concentration of furan compared to maleimide ($M/F < 1$) show a linear increase in modulus as bis-maleimide crosslinker is added, which corresponds to the stoichiometric increase in modulus ($E_0 \propto n_x^{-1} \propto M/F$). However, in systems with a higher concentration of bis-maleimides ($M/F > 1$), dangling maleimides are evident and serve as side-chain extenders to decrease modulus accordingly. In this study, we consider $M/F < 1$ where E_0 can be accurately controlled through crosslinker concentration (Figure 2C inset, dashed line). The corresponding crosslink densities varying from 4.7 to 18.9 mol m⁻³ were deduced from the Young's modulus using the recently developed network forensics methodology (Figure S15). The synthesized networks exhibited high gel fractions of $99.9 \pm 0.1\%$ due to (i) high crosslink efficiency of large size macromolecules and (ii) purification of brushes prior to crosslinking. However, the reported gel fraction might be overestimated because of extremely slow diffusion of bulky bottlebrushes in a polymer network with a mesh size smaller than individual macromolecules.

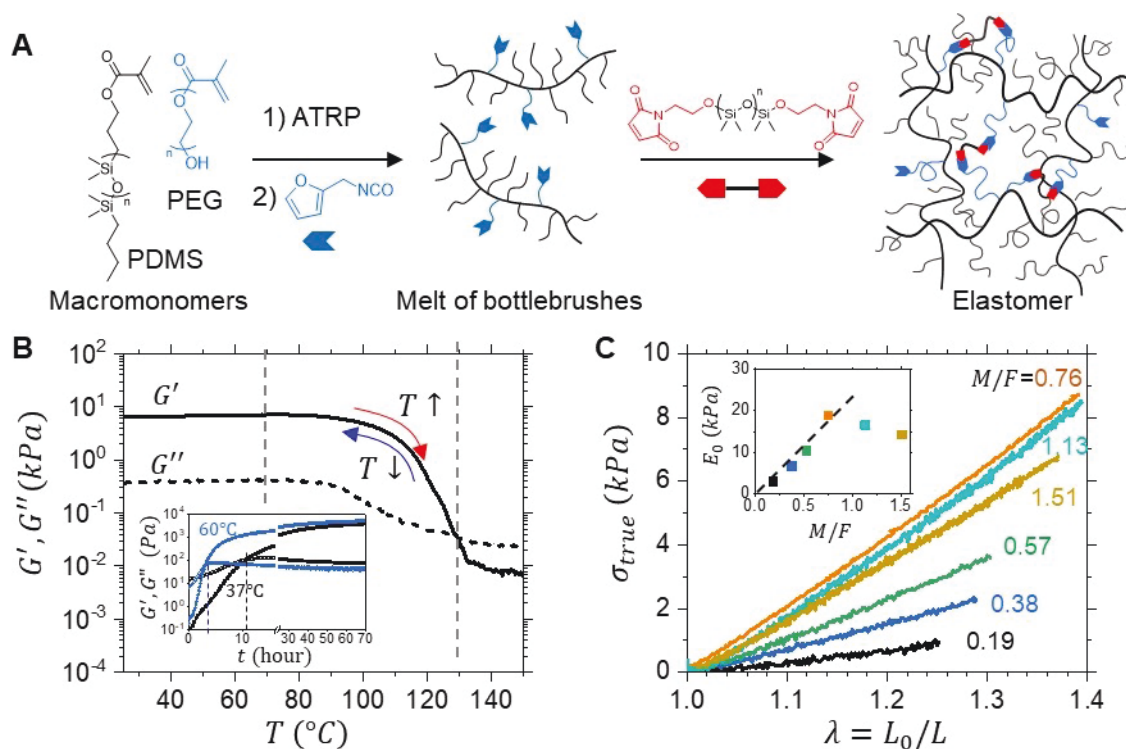


Figure 2. A) Synthesis of bottlebrush precursors followed by their crosslinking using the Diels–Alder (DA) coupling of furan (F) and maleimide (M) moieties. B) Monitoring reversible disassembly of a DA network upon heating (1 K min^{-1}) by measuring the storage (G') and loss (G'') moduli ($\varepsilon = 0.1, f = 0.1 \text{ Hz}$). Inset: time-dependent DA crosslinking of elastomer at two different temperatures: 37 and 60°C . C) Stress-elongation curves ($10^{-3} \text{ s}^{-1}, T = 24^\circ\text{C}$) of PDMS bottlebrush elastomers crosslinked with different M/F fractions (as indicated) of the maleimide (M) and furan (F) groups in bis-maleimide crosslinkers and PDMS side chains, respectively. Inset: Young's modulus (E_0) variation with the M/F ratio, where the dashed line corresponds to the theoretical E_0 expected from the M/F ratios. Initially up to $M/F \approx 1$, E_0 follows the crosslinking stoichiometry. At $M/F > 1$, a portion of bis-maleimides reacts only once resulting in side-chain extension, hence modulus decrease.

For closed-loop recycling of the DA-crosslinked elastomers, we exploit the ability of anthracene to react irreversibly with maleimide moieties (Figure 3A,B). To accomplish network disassembly, the crosslinked networks are preloaded with 9-anthracenemethanol and heated to 130°C , producing a free-flowing viscoelastic fluid (Figure 3C inset). Complete recovery of the polymer melt is achieved at a 9-anthracenemethanol concentration of 0.1 wt %, which represents a twofold excess of anthracene compared to furan groups (Supporting Information, Figure S7). The disassembly process is monitored by measuring the shear storage and loss moduli as a function of time at constant $T = 130^\circ\text{C}$ (Figure 3C, Figure S8). The anthracene-loaded network yields melt of lower G'' , which suggests lower molecular weight products of the disassembly process. To verify the capturing of maleimide moieties by anthracene, the melts were cooled down from 130 to 60°C to re-initiate DA cycloaddition. As expected, the formulation without anthracene rapidly ($< 180 \text{ sec}$) re-crosslinks to restore the original modulus value of $G' \approx 7 \text{ kPa}$ (Figure 3D). In contrast, the anthracene-loaded formulation does not re-crosslink ($G' < G''$) over a period of 15 days. As corroborated by NMR of urethane peaks (Supporting Information, Figure S9), the furan-containing polymer melts remain active and undergo DA cycloaddition with newly introduced cross-

linkers (Figure 3B) to enable reassembly of the elastomer with nearly identical dynamic and equilibrium mechanical properties compared to the original elastomer (Figure 3E and F).

Within the same framework, we hypothesized that it is possible to make elastomers softer or stiffer on demand through controlled addition of crosslinker scavengers (Figure 4A) or crosslinkers (Figure 4B), respectively. For elastomer softening, we prepared a series of anthracene-loaded samples with different sub-stoichiometric ratios of 9-anthracenemethanol to furan functional groups (0, 0.19, 0.38, 0.57). These elastomers remain stable at room temperature for a period of 12 days with no change in modulus (Supporting Information, Figure S10–S11). Upon heating to 80°C , the DA-crosslinks are rendered dynamic and a subset of maleimide groups reacts irreversibly with the anthracene functionality; thus, decreasing crosslink density without compromising the overall network integrity. The stability of the reconfigured network is verified by constant G' and G'' during $\approx 16 \text{ hrs}$ after decrosslinking (Supporting Information, Figure S11). Tensile experiments determine that the decrease in Young's modulus is precisely controlled by the relative concentration of anthracene (Figure 4C). For example, a $M/F = 0.76$ network loaded with 0.19 eq of anthracene became 25 % (0.19/0.76) softer compared with the original

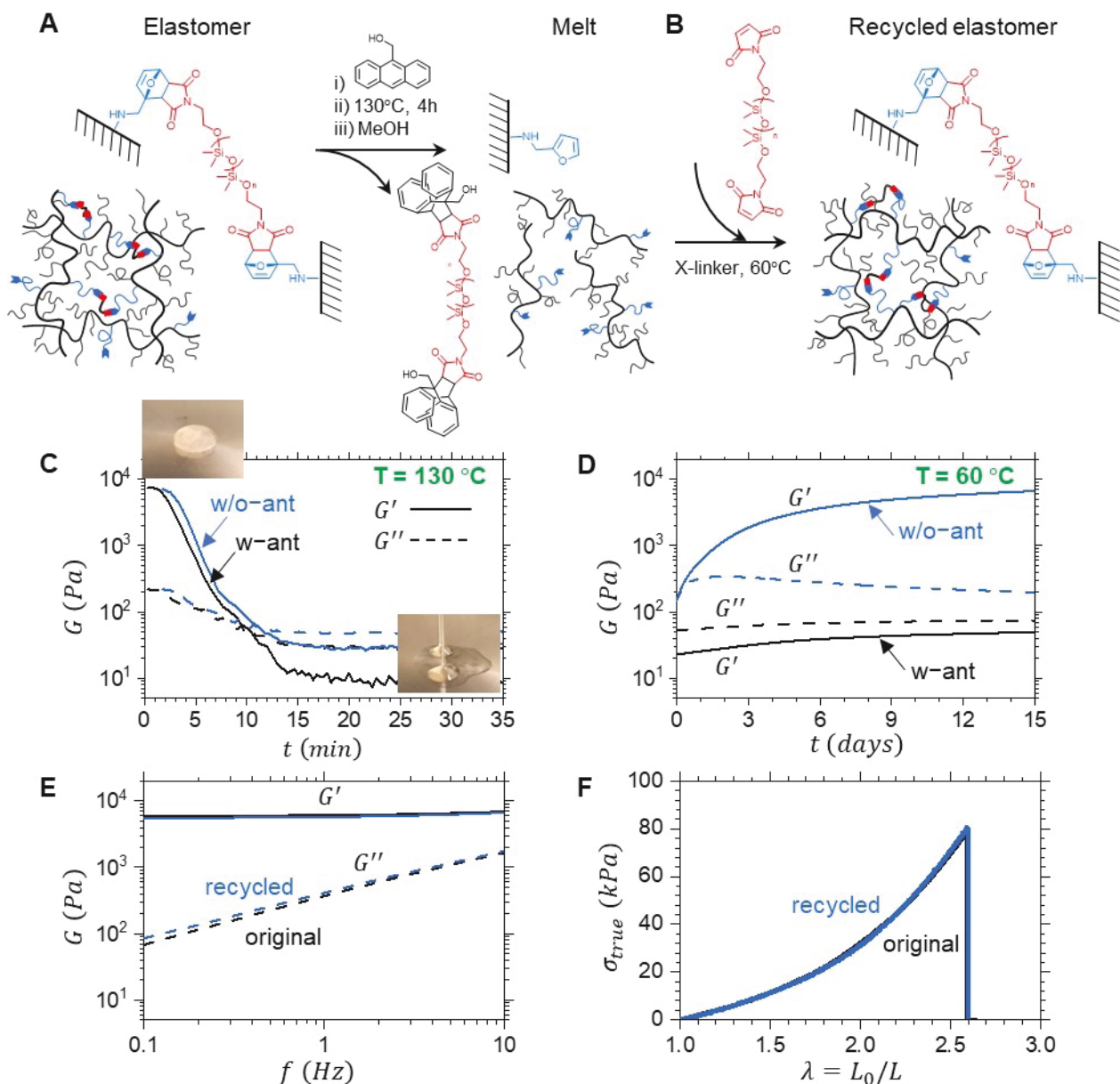


Figure 3. Recycling of bottlebrush elastomers. A) Transformation of bottlebrush networks into polymer melts upon heating to 130 °C in the presence of 9-anthracenemethanol (see Supporting Information for experimental details). B) Network re-assembly is implemented by addition of bis-maleimide crosslinkers to the disassembled polymer melt at 60 °C. C) Comparison of storage (G') and loss (G'') shear moduli variation at $T = 130$ °C for two samples with the same crosslink density ($M/F = 0.76$) loaded with anthracene (w-ant) and without anthracene (w/o-ant). Over a period of 35 minutes both samples are de-crosslinked. Insets: snapshots of anthracene-loaded samples before and after de-crosslinking. D) The corresponding moduli variation in presence and absence of anthracene during isothermal annealing of the recovered samples from C at 60 °C. Without anthracene, the elastomer regains its original stiffness, but the presence of anthracene maintains stability of the polymer melt. E) Rheological and F) tensile tests performed on the initial ($M/F = 0.76$) and recycled thermosets demonstrate nearly identical mechanical properties.

elastomer: $E_{0,0.19} = 0.75E_{0,0.76} = 0.75 \cdot 18.9 = 14.2$ kPa (Figure 4D).

For elastomer stiffening, the DA crosslinked brush elastomers are pre-loaded with different concentrations of furan protected bis-maleimides as inert, dormant crosslinkers (Figure 4B and Figure S12). Heating to 80 °C results in deprotection of maleimides through retro-DA and

simultaneous evaporation of furan ($b_p \approx 31$ °C), which enables the activated crosslinkers to react with the F-functionalized side chains. The reconfigured networks demonstrate a linear increase in crosslink density with the corresponding stoichiometric addition of crosslinker (Figure 4E,F and Supporting Information Figures S12–S13). For instance, a reconfigured sample $M/F = 0.38 + 0.19$, obtained by adding

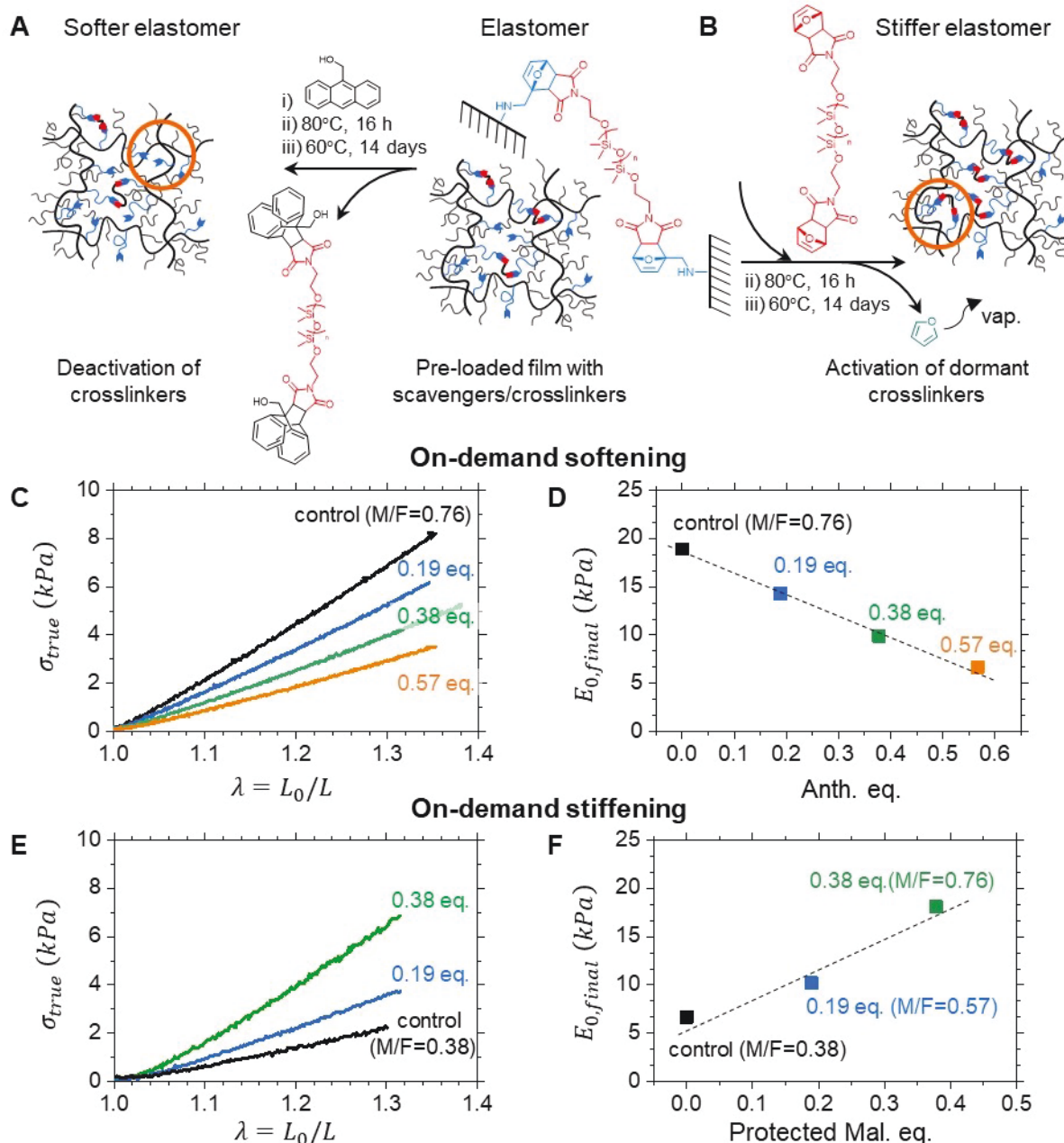


Figure 4. Switching stiffness on demand. A) For softening, a fully crosslinked bottlebrush elastomer is loaded with controlled amounts of 9-anthracenemethanol and heated up to 80 °C (resulting in partial decrosslinking) and then kept at 60 °C for network formation through remaining bis-maleimides. B) For elastomer stiffening, a partially crosslinked elastomer is loaded with different molar fractions of furan-protected bis-maleimide crosslinker. Dormant crosslinkers are deprotected upon heating to 80 °C followed by furan evaporation and cooling to 60 °C for network formation. C) Stress-elongation curves (10^{-3} s^{-1} , $T=24 \text{ }^{\circ}\text{C}$) and D) the corresponding Young's moduli of elastomers prepared according to route A with different molar fractions of 9-anthracenemethanol, as indicated. Control corresponds to a $M/F=0.76$ elastomer, while, e.g., 0.19 eq corresponds to $A/F=0.19$ molar fraction of anthracene moieties relative to furan-functionalized side chains. E) Stress-elongation curves and F) the corresponding Young's moduli of elastomers prepared according to route B with different fractions of dormant bis-maleimide crosslinker. The control sample is a $M/F=0.38$ bottlebrush elastomer, where 0.19 eq corresponds to $M/F=0.19$ molar fraction of dormant maleimides relative to furan chain-ends.

0.19 of dormant crosslinker to the original sample $M/F=0.38$ shows a modulus of 10.2 kPa (Figure 4F), which is nearly identical to 10.5 kPa of an original $M/F=0.57$ sample (Figure 2C). The stoichiometric control over modulus is corroborated by additional examples of the reconfigured $M/$

$F=0.38+0.38$ vs. original $M/F=0.76$ samples that show 18.1 kPa and 18.9 kPa, respectively.

Conclusion

In conclusion, we have demonstrated a versatile system, where mechanical properties of bottlebrush elastomers with thermoreversible Diels–Alder crosslinks can be either recycled or reconfigured within a pre-determined modulus range. Dormant crosslinkers and crosslink scavengers that are stable and inert during room temperature storage are used to alter the crosslink density upon thermal activation. The structural integrity of the network is preserved in this solvent-free process, which makes these tissue-like materials particularly useful in applications that would benefit from customizable mechanical properties, such as soft robotics, actuators, and personalized medical devices. Moreover, the elastomers can be converted to a melt of bottlebrush precursors and then reassembled on demand showing no property deterioration when compared to pristine elastomers. This provides a platform for circular materials that significantly reduce the prototype cost of the devices and boost their sustainability. Lastly, the reconfigurability and recyclability presented in this work are achieved by manipulating the crosslinking chemistry independent from the backbone or side chain chemistry, making this approach potentially applicable to a wide range of polymers.

Acknowledgements

The authors acknowledge funding from the National Science Foundation (DMR 1921835 and 2004048). A.V.B. acknowledges the Ministry of Science and Higher Education of the Russian Federation (Agreement No. 075-15-2020-794). F.A.L. acknowledges the National Institute of General Medical Sciences of the National Institute of Health (1-R35-GM142666-01).

Conflict of Interest

The authors declare no conflict of interest

Data Availability Statement

The data that support the findings of this study are available from the corresponding author upon reasonable request.

Keywords: Bottlebrush · Diels–Alder · Elastomers · Recycling · Upcycling

- [1] P. R. Christensen, A. M. Scheuermann, K. E. Loeffler, B. A. Helms, *Nat. Chem.* **2019**, *11*, 442–448.
- [2] M. A. Borden, F. A. Leibfarth, *Nat. Chem.* **2021**, *13*, 930–932.
- [3] M. Häußler, M. Eck, D. Rothauer, S. Mecking, *Nature* **2021**, *590*, 423–427.
- [4] L. S. T. J. Korley, T. H. Epps, B. A. Helms, A. J. Ryan, *Science* **2021**, *373*, 66–69.

- [5] B. D. Vogt, K. K. Stokes, S. K. Kumar, *ACS Appl. Polym. Mater.* **2021**, *3*, 4325–4346.
- [6] K. Ragaert, L. Delva, K. Van Geem, *Waste Manage.* **2017**, *69*, 24–58.
- [7] J. M. Eagan, J. Xu, R. Di Girolamo, C. M. Thurber, C. W. Macosko, A. M. La Pointe, F. S. Bates, G. W. Coates, *Science* **2017**, *355*, 814–816.
- [8] A. L. Kocen, S. Cui, T.-W. Lin, A. M. LaPointe, G. W. Coates, *J. Am. Chem. Soc.* **2022**, *144*, 12613–12618.
- [9] C. Vadenbo, S. Hellweg, T. F. Astrup, *J. Ind. Ecol.* **2017**, *21*, 1078–1089.
- [10] S. R. Nicholson, J. E. Rorrer, A. Singh, M. O. Konev, N. A. Rorrer, A. C. Carpenter, A. J. Jacobsen, Y. Román-Leshkov, G. T. Beckham, *Annu. Rev. Chem. Biomol. Eng.* **2022**, *13*, 301–324.
- [11] G. Xu, Q. Wang, *Green Chem.* **2022**, *24*, 2321–2346.
- [12] Y. Liu, Z. Yu, B. Wang, L. Pengyun, J. Zhu, S. Ma, *Green Chem.* **2022**, *24*, 5691–5807.
- [13] C. J. Kloxin, C. N. Bowman, *Chem. Soc. Rev.* **2013**, *42*, 7161–7173.
- [14] S. Oh, E. E. Stache, *J. Am. Chem. Soc.* **2022**, *144*, 5745–5749.
- [15] T. Tan, W. Wang, K. Zhang, Z. Zhan, W. Deng, Q. Zhang, Y. Wang, *ChemSusChem* **2022**, *15*, e202200522.
- [16] C. Jehanno, J. W. Alty, M. Roosen, S. De Meester, A. P. Dove, E. Y.-X. Chen, F. A. Leibfarth, H. Sardon, *Nature* **2022**, *603*, 803–814.
- [17] T. J. Fazekas, J. W. Alty, E. K. Neidhart, A. S. Miller, F. A. Leibfarth, E. J. Alexanian, *Science* **2022**, *375*, 545–550.
- [18] M. Olszewski, L. Li, G. Xie, A. Keith, S. S. Sheiko, K. Matyjaszewski, *J. Polym. Sci. Part A* **2019**, *57*, 2426–2435.
- [19] C. M. Plummer, L. Li, Y. Chen, *Polym. Chem.* **2020**, *11*, 6862–6872.
- [20] M. L. Lepage, C. Simhadri, C. Liu, M. Takaffoli, L. Bi, B. Crawford, A. S. Milani, J. E. Wulff, *Science* **2019**, *366*, 875–878.
- [21] J. B. Williamson, S. E. Lewis, R. R. Johnson, I. M. Manning, F. A. Leibfarth, *Angew. Chem. Int. Ed.* **2019**, *58*, 8654–8668; *Angew. Chem.* **2019**, *131*, 8746–8761.
- [22] J. B. Williamson, C. G. Na, R. R. Johnson, W. F. M. Daniel, E. J. Alexanian, F. A. Leibfarth, *J. Am. Chem. Soc.* **2019**, *141*, 12815–12823.
- [23] S. E. Lewis, B. E. Wilhelmy, F. A. Leibfarth, *Chem. Sci.* **2019**, *10*, 6270–6277.
- [24] S. Ügdüler, K. M. Van Geem, M. Roosen, E. I. P. Delbeke, S. De Meester, *Waste Manage.* **2020**, *104*, 148–182.
- [25] T. W. Walker, N. Frelka, Z. Shen, A. K. Chew, J. Banick, S. Grey, M. S. Kim, J. A. Dumesic, R. C. Van Lehn, G. W. Huber, *Sci. Adv.* **2020**, *6*, eaba7599.
- [26] X. Liu, M. Hong, L. Falivene, L. Cavallo, E. Y. X. Chen, *Macromolecules* **2019**, *52*, 4570–4578.
- [27] B. R. Elling, W. R. Dichtel, *ACS Cent. Sci.* **2020**, *6*, 1488–1496.
- [28] M. Röttger, T. Domenech, R. Van Der Weegen, A. Breuillac, R. Nicolaÿ, L. Leibler, *Science* **2017**, *356*, 62–65.
- [29] D. J. Fortman, J. P. Brutman, C. J. Cramer, M. A. Hillmyer, W. R. Dichtel, *J. Am. Chem. Soc.* **2015**, *137*, 14019–14022.
- [30] T. Rogge, N. Kaplaneris, N. Chatani, J. Kim, S. Chang, B. Punji, L. L. Schafer, D. G. Musaev, J. Wencel-Delord, C. A. Roberts, R. Sarpong, Z. E. Wilson, M. A. Brimble, M. J. Johansson, L. Ackermann, *Nat. Rev. Methods Primers* **2021**, *1*, 43.
- [31] N. Vora, P. R. Christensen, J. Demarteau, N. R. Baral, J. D. Keasling, B. A. Helms, C. D. Scown, *Sci. Adv.* **2021**, *7*, eabf0187.
- [32] G. M. Scheutz, J. J. Lessard, M. B. Sims, B. S. Sumerlin, *J. Am. Chem. Soc.* **2019**, *141*, 16181–16196.
- [33] M. J. Webber, M. W. Tibbitt, *Nat. Rev. Mater.* **2022**, *7*, 541–556.
- [34] J. Demarteau, A. R. Epstein, P. R. Christensen, M. Abubekrov, H. Wang, S. J. Teat, T. J. Seguin, C. W. Chan, C. D. Scown,

- T. P. Russell, J. D. Keasling, K. A. Persson, B. A. Helms, *Sci. Adv.* **2022**, *8*, abp8823.
- [35] M. Vatankehah-Varnosfaderani, A. N. Keith, Y. Cong, H. Liang, M. Rosenthal, M. Sztucki, C. Clair, S. Magonov, D. A. Ivanov, A. V. Dobrynin, S. S. Sheiko, *Science* **2018**, *359*, 1509–1513.
- [36] C. Clair, A. Lallam, M. Rosenthal, M. Sztucki, M. Vatankehah-Varnosfaderani, A. N. Keith, Y. Cong, H. Liang, A. V. Dobrynin, S. S. Sheiko, D. A. Ivanov, *ACS Macro Lett.* **2019**, *8*, 530–534.
- [37] J. M. Sarapas, E. P. Chan, E. M. Rettner, K. L. Beers, *Macromolecules* **2018**, *51*, 2359–2366.
- [38] S. S. Sheiko, F. Vashahi, B. J. Morgan, M. Maw, E. Dashtimoghadam, F. Fahimipour, M. Jacobs, A. N. Keith, M. Vatankehah-Varnosfaderani, A. V. Dobrynin, *ACS Cent. Sci.* **2022**, *8*, 845–852.
- [39] B. B. Patel, D. J. Walsh, D. H. Kim, J. Kwok, B. Lee, D. Guironnet, Y. Diao, *Sci. Adv.* **2020**, *6*, 7202–7212.
- [40] F. Vashahi, M. R. Martinez, E. Dashtimoghadam, F. Fahimipour, A. N. Keith, E. A. Bersenev, D. A. Ivanov, E. B. Zhulina, P. Popryadukhin, K. Matyjaszewski, M. Vatankehah-Varnosfaderani, S. S. Sheiko, *Sci. Adv.* **2022**, *8*, abm2469.
- [41] E. Dashtimoghadam, F. Fahimipour, A. N. Keith, F. Vashahi, P. Popryadukhin, M. Vatankehah-Varnosfaderani, S. S. Sheiko, *Nat. Commun.* **2021**, *12*, 3961.
- [42] R. Xie, S. Mukherjee, A. E. Levi, V. G. Reynolds, H. Wang, M. L. Chabiny, C. M. Bates, *Sci. Adv.* **2020**, *6*, eabc6900.
- [43] C. Choi, J. L. Self, Y. Okayama, A. E. Levi, M. Gerst, J. C. Speros, C. J. Hawker, J. Read De Alaniz, C. M. Bates, *J. Am. Chem. Soc.* **2021**, *143*, 9866–9871.
- [44] E. H. Discekici, A. H. St. Amant, S. N. Nguyen, I. H. Lee, C. J. Hawker, J. Read De Alaniz, *J. Am. Chem. Soc.* **2018**, *140*, 5009–5013.
- [45] A. P. Bapat, J. G. Ray, D. A. Savin, E. A. Hoff, D. L. Patton, B. S. Sumerlin, *Polym. Chem.* **2012**, *3*, 3112–3120.
- [46] E. M. Foster, E. E. Lensmeyer, B. Zhang, P. Chakma, J. A. Flum, J. J. Via, J. L. Sparks, D. Konkolewicz, *ACS Macro Lett.* **2017**, *6*, 495–499.
- [47] S. Terryn, J. Brancart, E. Roels, R. Verhelle, A. Safaei, A. Cuvellier, B. Vanderborgh, G. Van Assche, *Macromolecules* **2022**, *55*, 5497–5513.
- [48] K. J. Luo, L. B. Huang, Y. Wang, J. R. Yu, J. Zhu, Z. M. Hu, *Chin. J. Polym. Sci.* **2020**, *38*, 268–277.
- [49] H. Chang, M. S. Kim, G. W. Huber, J. A. Dumesic, *Green Chem.* **2021**, *23*, 9479–9488.
- [50] X. Kuang, G. Liu, X. Dong, X. Liu, J. Xu, D. Wang, *J. Polym. Sci. Part A* **2015**, *53*, 2094–2103.
- [51] L. M. Polgar, M. Van Duin, A. A. Broekhuis, F. Picchioni, *Macromolecules* **2015**, *48*, 7096–7105.
- [52] Q. Zhou, Z. Sang, K. K. Rajagopalan, Y. Sliozberg, F. Gardea, S. A. Sukhishvili, *Macromolecules* **2021**, *54*, 10510–10519.

Manuscript received: December 6, 2022

Accepted manuscript online: December 30, 2022

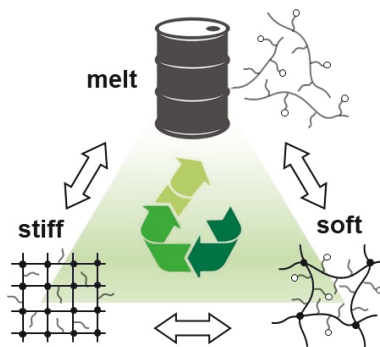
Version of record online: ■■■

Research Articles

Bottlebrush Polymers

D. Zhang, F. Vashahi, E. Dashtimoghadam, X. Hu, C. J. Wang, J. Garcia, A. V. Bystrova, M. Vatankhah-Varnoosfaderani, F. A. Leibfarth, S. S. Sheiko* . e202217941

Circular Upcycling of Bottlebrush Thermosets



Built-in circularity by integrating closed-loop recycling and upcycling in brush-like thermosets with dynamic crosslinks.